JOURNAL OF VIROLOGY, Aug. 1994, p. 4747–4758
0022-538X/94/$04.00+0

Vol. 68, No. 8

Strand Displacement Synthesis Capability of Moloney Murine Leukemia Virus Reverse Transcriptase

SAMUEL H. WHITING AND JAMES J. CHAMPOUX*

Department of Microbiology, School of Medicine, University of Washington, Seattle, Washington 98195

Received 10 March 1994/Accepted 21 April 1994

The accepted model of retroviral reverse transcription includes a circular DNA intermediate which requires strand displacement synthesis for linearization and creation of an integration-competent, long terminal repeat-flanked DNA product. We have used an in vitro model of this last step of reverse transcription to examine the role of the viral enzyme, reverse transcriptase (RT), in displacement synthesis. We show that Moloney murine leukemia virus RT possesses an activity which allows for displacement synthesis through a minimum of 1,334 bp of duplex DNA—an extent much greater than that required during in vivo reverse transcription and over 25-fold greater than has been previously demonstrated for a viral RT. RT does not function as a helicase in the classical sense but appears to closely couple duplex DNA melting with synthesis-driven translocation of the enzyme. In the absence of synthesis, the unwound region created by a primer-positioned RT appears to be no greater than 2 bp and does not advance along the template. Additionally, RT does not utilize ATP or any deoxynucleoside triphosphate not directly encoded by the template strand to catalyze processive duplex unwinding at a nick; nor does binding of the enzyme unwind duplex DNA in the absence of a 3′ terminus. The approximate maximum chain elongation rate during strand displacement synthesis by Moloney murine leukemia virus RT falls between 0.73 and 1.5 nucleotides per s at 37°C. The RNase H activity of RT does not appear to play a role in displacement synthesis; however, a 181-amino-acid C-terminal truncation of RT displays a dramatically reduced ability to catalyze synthesis through duplex DNA.

The retroviral reverse transcriptase (RT) catalyzes the conversion of the single-stranded viral RNA genome into a double-stranded, terminally redundant DNA molecule. After a specific tRNA-primed initiation event near the 5′ end of the positive-sense RNA genome, reverse transcription proceeds through an intricate series of steps, including two independent "jumps," or strand transfer reactions, to produce full-length minus and plus DNA strands; in the process, sequences unique to the 5′ and 3′ ends of the genome are duplicated to generate the long terminal repeat (LTR) regions of the final product (43). At least two enzymatic activities of RT are required for reverse transcription. The protein functions as both an RNA- and DNA-directed DNA polymerase and also possesses an RNase activity specific for RNA-DNA hybrid duplexes (RNase H) (43). Despite this multiplicity of activities, not all functions required during reverse transcription have, to date, been demonstrated to reside within RT. In particular, while it is clear that strand displacement synthesis is necessary for completion of reverse transcription (see Fig. 1) (15), the mechanism for achieving displacement synthesis to the extent required in vivo has not been determined.

Early evidence for the occurrence of strand displacement synthesis during endogenous reverse transcription was obtained when linear viral DNA was examined in the avian sarcoma-leukosis virus (ASLV) system. It was noted in both permeabilized virions and in infected cells that while the viral minus-strand DNA was predominantly genome length, plus strands were discontinuous, being composed of multiple subgenomic fragments (3, 19, 23, 40). Both biochemical (3, 19, 40) and electron microscopic (23) analyses demonstrated that the discontinuous plus strands were characterized by the presence of multiple single-stranded branches. These data led to the generation of a model whereby, in at least one retrovirus system, multiple initiation events during plus-strand synthesis lead to a minimum partial displacement of downstream plus strands by those originating upstream (3, 23). Similarly, the potential for strand displacement during the synthesis of human immunodeficiency virus type 1 (HIV-1) plus strands follows from the discovery of a second, upstream, polypurine tract (PPT) that, in addition to the normal PPT (8), provides a site for the initiation of plus strands (9, 10). The most easily defined requirement for displacement synthesis occurs following the second strand transfer reaction of reverse transcription. In this step, complementary sequences found at the 3′ ends of the nascent plus and minus DNA strands pair intramolecularly to form a circular intermediate (20) (Fig. 1, second jump). Subsequent extension of the 3′ terminus of the minus-strand DNA, which is required for LTR generation and linearization of the intermediate, must proceed through a relatively long stretch of duplex DNA: in Moloney murine leukemia virus (M-MuLV), the LTR region is 594 bp (38); in HIV-1, it is 636 bp (32).

Previous work has suggested that at least two retroviral RTs possess a limited ability to promote strand displacement synthesis. The purified avian myoblastosis virus (AMV) RT was reported to have a DNA-DNA duplex and an RNA-DNA hybrid duplex unwinding-like activity (11), and independently, it was found to catalyze roughly 45 to 55 bp of displacement synthesis on nicked, double-stranded DNA templates (30). Purified HIV-1 RT was shown to catalyze limited displacement synthesis, in vitro, up to a maximum of approximately 50 bp (18, 21).

Because these demonstrated activities are roughly 10-fold less than the expected requirement for in vivo reverse transcription, the precise mechanism of in vivo strand displacement synthesis remains unclear. It is distinctly possible that additional viral proteins present in the subviral nucleoprotein

* Corresponding author. Mailing address: Dept. of Microbiology SC-42, University of Washington, Seattle, WA 98195. Phone: (206) 543-8574. Fax: (206) 543-8297.

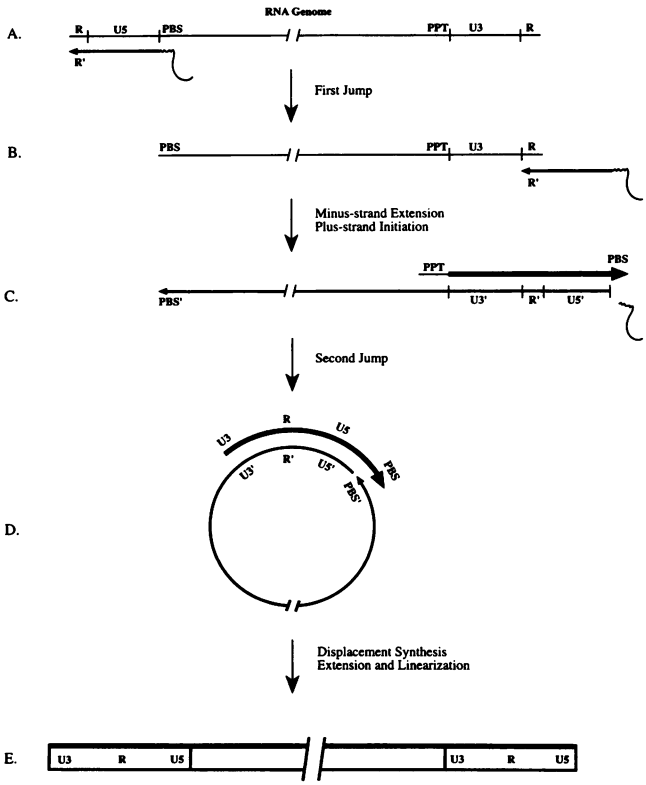

FIG. 1. Retroviral Reverse Transcription. (A) Reverse transcription begins near the 5′ end of the viral plus-strand RNA genome. Primed by a host transfer-RNA molecule which base pairs with the RNA template at the primer binding site (PBS), minus-strand DNA synthesis proceeds to the 5′ end of the viral RNA. (B) Following RNase H degradation of the RNA, translocation (the first jump) of the nascent DNA strand to the 3′ end of the same or the second RNA genome is mediated by base pairing between the complementary R sequences. (C) Continuation of minus-strand DNA synthesis is accompanied by degradation of the RNA. At the PPT directly adjacent to the U3 region of the genome, a specific RNase H-mediated cleavage of the RNA strand creates a primer for initiation of plus-strand DNA; the plus strand is extended into the PBS region of the tRNA, and the tRNA is removed by RNase H. (D) In the second jump, the 3′ end of the nascent plus strand base pairs intramolecularly to a complementary sequence at the 3′ end of the minus-strand DNA to generate a circular intermediate. (E) Extension of both the plus-strand and the minus-strand DNAs, accompanied by strand displacement through at least the LTR region, completes the viral LTR sequences and linearizes the circular molecule to form the complete, preintegrative, double-stranded DNA product.

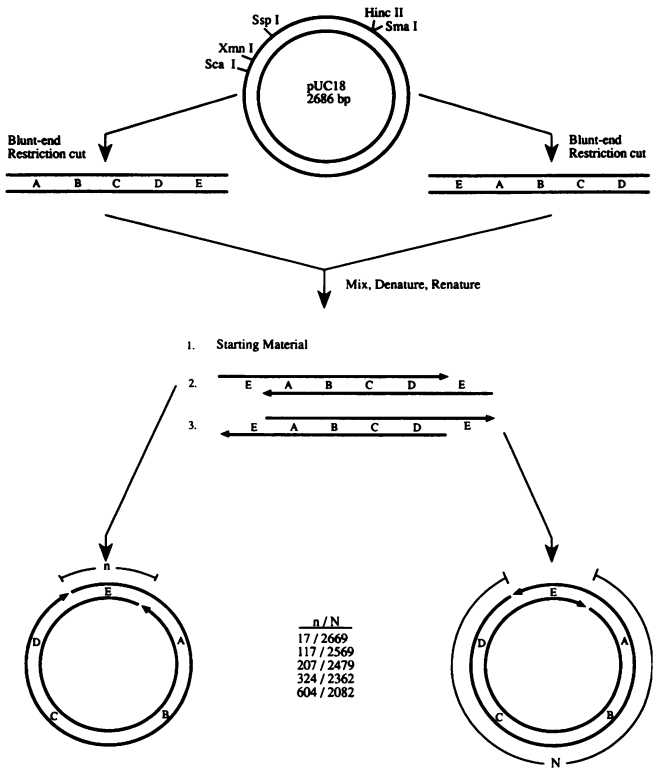

FIG. 2. Preparation of displacement synthesis templates. Pairs of pUC18 linear molecules generated by restriction enzyme digestion were mixed, denatured, and renatured as described in Materials and Methods. As shown, each annealing reaction produced two templates. The labels n and N correspond to the amount of duplex DNA through which displacement synthesis is primed and are used to designate a given template pair. The arrowheads indicate the positions of 3′-hydroxyls and the direction of primed synthesis. The enzymes used to produce each template pair were: 17/2669, *Sma*I and *Hinc*II; 117/2569, *Sca*I and *Xmn*I; 207/2479, *Xmn*I and *Ssp*I; 324/2362, *Ssp*I and *Sca*I; and 604/2082, *Ssp*I and *Hinc*II.

complex, or host factors present in the cytoplasm, facilitate displacement synthesis by RT. We have readdressed the capacity of RT to catalyze displacement of the nontemplate strand during DNA synthesis by utilizing purified M-MuLV RT and DNA templates designed to approximate the intermediate created by the second strand transfer of reverse transcription. In this model system we have demonstrated that purified M-MuLV RT can carry out displacement synthesis on a duplex DNA template in vitro to an extent that is clearly greater than what is required in vivo.

MATERIALS AND METHODS

Recombinant M-MuLV RT was purchased from GIBCO-BRL (Life Technologies, Inc.) and, where indicated, from United States Biochemical Corp. The RNase H^- mutant forms of M-MuLV RT, Superscript I and II, and mung bean nuclease were from GIBCO-BRL. All restriction endonucleases were purchased from New England Biolabs, Inc. Recombinant human topoisomerase I was purified from baculovirus-infected insect cells by a procedure which will be detailed elsewhere. [α-^{32}P]dATP (3,000 Ci/mmol) was purchased from Dupont NEN Research Products, and deoxynucleoside triphosphates (dNTPs) were from Pharmacia Biotech, Inc. Supplies for electron microscopy were from Ted Pella, Inc. pUC18 plasmid DNA was isolated from transformed DH5α cells by the alkaline lysis method (1) and purified by centrifugation through two sequential CsCl-ethidium bromide density gradients. pBluescript II KS(+) plasmid DNA (Stratagene) was purified with a Qiagen Plasmid Maxi Kit by following the directions of the manufacturer.

Preparation of circular displacement templates. Linear preparations of pUC18 DNA were generated with the single-cut restriction endonucleases *Hinc*II, *Sca*I, *Sma*I, *Ssp*I, and *Xmn*I. Paired combinations of blunt-end linear molecules were used to generate the displacement templates shown in Fig. 2. The resulting template pairs are designated n/N, according to the amount of duplex DNA through which displacement synthesis is primed. A mixture containing 0.5 μg of each linear

molecule of a given pair was denatured in 0.2 M NaOH (final volume, 76 μl) for 10 min at room temperature. The sample was chilled on ice, brought to 50 mM Tris-HCl (pH 8.0), and neutralized with HCl (final pH 7.2 to 7.6; volume, 100 μl) before being annealed at 60°C (templates 117/2569, 207/2479, 324/2362, and 604/2082) or 45°C (templates 17/2669) for 1.5 h. After annealing, the samples were loaded on a 1% vertical Tris-borate-EDTA (TBE) agarose gel (1) (FMC Bioproducts; Seakem GTG agarose) and electrophoresed at 1.7 V/cm for approximately 16 h to separate nicked from linear molecules. The DNA loading buffer was 4% Ficoll, 0.03% bromphenol blue, 0.03% xylene cyanole, and 2 mM EDTA. The DNA bands corresponding to nicked circles (form II) were cut out, and the DNA was eluted from the gel slices and purified by two phenol extractions, two chloroform extractions, and precipitation with 2 volumes of ethanol in the presence of 0.3 M sodium acetate.

RT-mediated displacement synthesis. The reaction (final volume, 30 μl) contained 180 ng of template DNA (0.1 pmol) in 50 mM Tris-HCl (pH 8.3), 50 mM KCl, 6 mM $MgCl_2$, 10 mM dithiothreitol (DTT), and 0.2 mM dNTPs. Synthesis was initiated by the addition of 1 μl of RT (200 U; approximately 7 pmol), and the reaction mixtures were incubated for 3 h at 37°C. The reactions were terminated by the addition of 1 μl of 0.5 M EDTA and extracted with 1 volume of phenol-chloroform-isoamyl alcohol (25:24:1) before electrophoresis on a 1% TBE-agarose gel. During the course of these experiments, trace levels of a nuclease and *Escherichia coli* topoisomerase I were detected in some lots of commercially supplied recombinant RT preparations. However, RT lots free of these contaminating activities exhibited identical levels of strand displacement activity.

[α-^{32}P]dATP-labeled time course of displacement synthesis. Template DNA (approximately 10 to 15 ng) was incubated for 3 min at 37°C in 50 mM Tris-Cl (pH 8.3), 50 mM KCl, 6 mM $MgCl_2$, 10 mM DTT, 0.9 μM [α-^{32}P]dATP (3,000 Ci/mmol), 14.1 μM unlabeled dATP, and 15 μM concentrations of dCTP, dGTP, and dTTP (volume, 29 μl). The reactions were initiated by the addition of 1 μl of RT (200 U) and incubated at 37°C. At the time points indicated in the figure legends, 2.5 μl of the reaction mixture was terminated by addition to 7.5 μl of stop solution (final concentration, 32 mM EDTA, 0.2% sodium dodecyl sulfate [SDS]). Samples were electrophoresed at ~2 V/cm for 16 h on a 1% TBE-agarose gel adjacent to unlabeled marker DNAs (form II, linear and molecular weight standards). The gel was stained with 0.5 μg of ethidium bromide per ml, and dried under vacuum, and the marker DNAs were visualized with UV irradiation. Phosphorescent indicators were used to mark the positions of the unlabeled marker DNAs before exposing the gel for autoradiography.

Mung bean nuclease treatment of displacement intermediates. The reaction conditions were identical to those described above for the labeled time course analysis. At the time points indicated in the figure legends, 7 μl of the reaction mixture was terminated by addition to 33 μl of 40 mM EDTA. The DNA was precipitated with 2 volumes of ethanol in the presence of 20 μg of tRNA per ml and 0.3 M sodium acetate. The pellet was resuspended in 48 μl of 50 mM sodium acetate (pH 5.0), 250 mM NaCl, 0.5 mM $ZnSO_4$, 1 mM L-cysteine, and 25% glycerol and divided equally into two new Eppendorf tubes. Mung bean nuclease-treated samples received 0.045 U (1 μl of a 1:1,000 dilution) of mung bean nuclease, while controls received 1 μl of H_2O. The samples were incubated for 20 min at 37°C before being stopped with 0.2% SDS and loaded on a 1% TBE-agarose gel.

Electron microscopy of displacement intermediates. The DNA synthesis reaction mixture contained 100 ng of the 207/2479 template DNA and 200 U of RT in 30 μl of 50 mM Tris-HCl (pH 8.3), 50 mM KCl, 6 mM $MgCl_2$, 10 mM DTT, and 0.2 mM dNTPs. After a 30-min incubation at 37°C, 18 μl of the reaction mixture was stopped with 1 μl of 0.5 mM EDTA for visualization on an agarose gel. The remaining 12 μl was spread by a formamide tray-spreading technique essentially as described by Davis et al. (12). In brief, the DNA was spread at 0.5 μg/ml in a 70-μl hyperphase containing 100 mM Tris-HCl (pH 8.5), 10 mM EDTA, 0.1 mg of cytochrome c, per ml, 8.6 mM KCl, 1 mM $MgCl_2$, 1.7 mM DTT, 30 μM dNTPs, and 40% formamide onto a hypophase of 10 mM Tris-HCl (pH 8.5), 1 mM EDTA, and 10% formamide. The film was allowed to form for 1 to 2 min and was then picked up onto freshly prepared (<24 h) 3% collodion-coated grids, stained for 30 s with 50 μM uranyl acetate in 90% ethanol, and rinsed for 10 s in 2-methylbutane. The grids were rotary shadowed with Pt/Pd at an 8° angle and carbon coated before examination on a JEOL 1200EXII transmission electron microscope at an 80 KV accelerating voltage.

Duplex-DNA unwinding assay with 17 template DNA. The 17 template was prepared through the annealing step as described above. After annealing (without separating linear and circular molecules), the DNA was concentrated and desalted with a Centricon 30 microconcentrator (Amicon) by following the instructions of the manufacturer. The final concentrated DNA was linearized with either *Sca*I or *Ssp*I and purified by phenol-chloroform-isoamyl alcohol (25:24:1) extraction and then by chloroform-isoamyl alcohol (24:1) extraction. The linear DNA was once again concentrated and desalted (dilution into 10 mM Tris-HCl [pH 7.6], 1 mM EDTA [TE]) with a Centricon 30 microconcentrator. A stock solution containing a 1:1 mix of the two linear DNAs (approximately 1.6 μg total, and 800 ng of displacement templates), 50 mM Tris-HCl (pH 8.3), 50 mM KCl, 6 mM $MgCl_2$, and 10 mM DTT was prepared and aliquoted for each of the reactions shown in Fig. 8, lanes 2 to 9. Nucleotide triphosphates and RT were added as indicated in the figure; the reactions were carried out in a final volume of 20 μl at 37°C for 30 min before termination with 10 mM EDTA. For the positive control, the DNA mixture was melted by heating to 55°C in TE.

Duplex-DNA unwinding assay in the absence of a primer terminus. Individual reaction mixtures contained 650 ng (0.33 pmol) of pBluescript II KS(+) DNA in 50 mM Tris-HCl (pH 8.3), 50 mM KCl, 6 mM $MgCl_2$, and 10 mM DTT in a final volume of 20 μl. Binding was initiated by adding RT (United States Biochemical M-MuLV RT or GIBCO-BRL Superscript II, as indicated) to the molar excess (enzyme-DNA) indicated in the figure legends, followed by incubation for 10 min at 37°C. Negative control reaction mixtures received bovine serum albumin (BSA) rather than RT at a 90:1 molar excess. T7 RNA polymerase binding was carried out at a 10:1 molar excess in 40 mM Tris-HCl (pH 7.5), 10 mM $MgCl_2$, 5 mM DTT, 0.2 mM GTP, and 50 μg of BSA per ml (1). Relaxation of supercoils was initiated by adding 1 μl (100 ng) of human topoisomerase I and continuing the incubation for 15 min at 37°C. Reactions were stopped with 4 μl of 1.5% SDS, and mixtures were extracted with 1 volume of phenol-chloroform-isoamyl alcohol (25:24:1) and then by 1 volume of chloroform-isoamyl alcohol (24:1). The samples were electrophoresed at 1.25 V/cm for 18 h on a 1.2% TBE-agarose gel in the presence of 0.5 μg of chloroquine per ml.

RESULTS

M-MuLV RT is capable of strand displacement synthesis through extensive regions of duplex DNA. We wished to test whether purified M-MuLV RT was sufficient to carry out concomitant DNA synthesis and displacement of the nontemplate strand over the distance required for completion of the LTRs during the terminal step of reverse transcription. To this end, a series of pUC18-based templates was constructed to approximate the circular structure produced by the second jump of reverse transcription. The templates were designed to prime synthesis through regions of duplex DNA ranging from 17 bp—a positive control based on the published ability of HIV-1 RT to catalyze 50 bp of displacement synthesis (18, 21)—through a maximum of 2,669 bp. As shown schematically in Fig. 2, pairs of unit-length linear molecules produced by cutting pUC18 with different single-site restriction enzymes were mixed, denatured and renatured to yield circular molecules containing single-strand breaks on opposing strands. The distance separating the breaks was determined by the particular pair of restriction enzymes used (see the legend of Fig. 2). Because of the two possible ways that the single strands could sort, one annealing reaction generated two templates which were identical but for the orientation of their 3′ termini (arrows in Fig. 2) and therefore the direction and extent of displacement synthesis primed from the two nicks. Each template pair will be referred to by numbers (n/N) indicating the amount of duplex DNA through which displacement synthesis is primed (n = short, N = long).

Similar to in vivo reverse transcription, in vitro DNA synthesis through the duplex region of a doubly nicked circular template described above would be expected to produce two results: (i) linearization of the DNA, and (ii) terminal duplication of the sequences through which displacement synthesis proceeds. Figure 3 shows an ethidium bromide-stained agarose gel containing the products of in vitro synthesis by M-MuLV RT for 3 h with the various displacement templates. Lane 1 shows the migration of linear pUC18, which is equivalent to opening of the circular DNA template without synthesis. Lanes 2 to 6 show the products of RT-catalyzed synthesis on the templates (indicated in the figure by only the shorter of the two displacement distances). Templates 17, 117, 207, 324, and 604 yielded a series of linear products with lengths that increased by the amounts predicted for displacement synthesis. Templates 2669, 2569, 2479, 2362, and 2082 also yielded linear products of the predicted sizes; in this case the series decreased in size by the expected amounts. The identity of two representative linear products (from the 604 and 2082 templates) was further confirmed by restriction analysis (data not shown). Lanes 7 through 11 show templates subjected to identical conditions minus RT and serve to mark the migration of the nicked circular starting templates. It is clear that for each template, RT was able to successfully catalyze strand displacement synthesis. With the 2669 template this corresponded to a minimum of 1,334 bp of displacement synthesis, assuming extension occurred from both nicks. The appearance of less product from the long templates than from the short templates suggests that RT is more likely to be stalled or slowed during synthesis through extensive stretches of duplex DNA. An inhibition of synthesis by the displaced single strands could account for this result (36).

Time course analysis of displacement synthesis reactions. A time course of displacement synthesis in the presence of [α-^{32}P]dATP was employed to examine the synthesis reactions in more detail. Figure 4 shows the results of one such experiment using the 604/2082 template pair. Consistent with the expectation that displacement synthesis intermediates should be nicked circular molecules with growing single-stranded tails, the time course was characterized by a population of ^{32}P-labeled molecules of decreasing electrophoretic mobility and increasing heterogeneity (lanes 1 to 10). Distinct

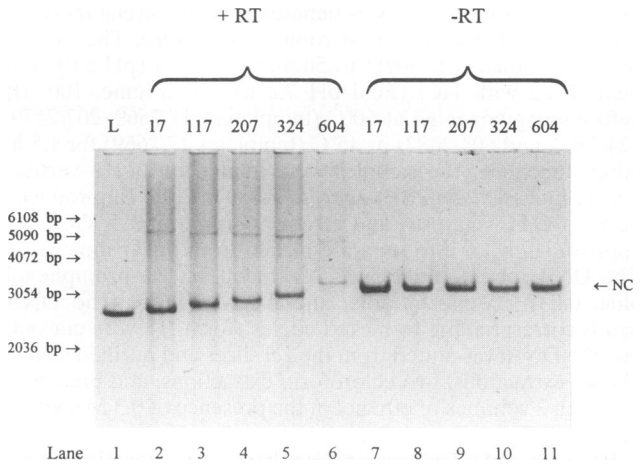

FIG. 3. Agarose gel analysis of displacement synthesis by RT. Synthesis by RT on the indicated template pairs (only the shorter of the two displacement distances is given) was for 3 h at 37°C (lanes 2 to 6). Lanes 7 to 11 were the corresponding controls incubated without RT. The agarose gel was stained with ethidium bromide, and the photographic negative is shown. Lane 1 contained linearized pUC18 DNA (L). NC marks the mobility of the nicked circular template. The positions of size markers are indicated at the left. The extra bands appearing in the negative control for the 17/2669 templates (lane 7) are probably faster-migrating complex knotted structures and more slowly migrating catenated molecules that result from the relative ease with which these two templates (held in circular form by only 17 bp) can open and reanneal.

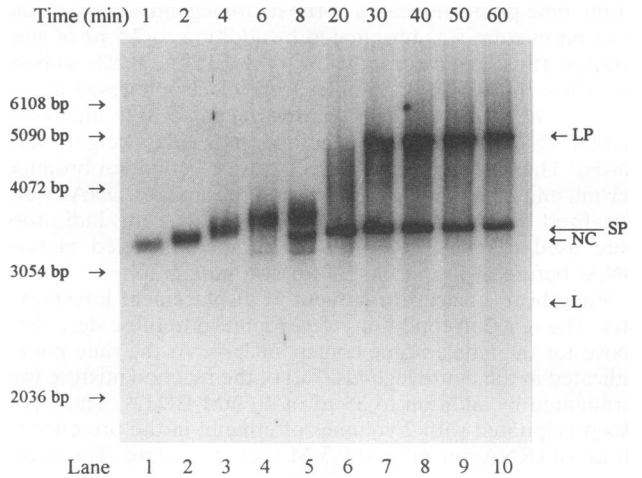

FIG. 4. Kinetics of displacement synthesis with ^{32}P-labeled dATP. RT-mediated synthesis on the 604/2082 template pair was performed in the presence of [α-^{32}P]dATP. Aliquots were stopped at the indicated times, and the samples were analyzed by agarose gel electrophoresis and then by autoradiography. Indicated on the right are the mobilities of the products of displacement synthesis on the 2082 template (LP, for long product) and the 604 template (SP, for short product); also indicated are the mobilities of the nicked circular DNA (NC) and linears (L).

TABLE 1. Rate of RT synthesis on displacement templates[a]

Template	Synthesis (nucleotides/s)	
	Unidirectional[b]	Bidirectional[c]
604	1.26–1.68	0.63–0.84
2082	1.33–1.44	0.66–0.72
2479	1.47–1.59	0.74–0.80
2669	1.48[d]	0.74[d]
Mean ± SD	1.46 ± 0.14	0.73 ± 0.07

[a] Rates were calculated on the basis of the known amount of displacement synthesis required and a time course "bracketing" of the first appearance of the linear product marking the completion of synthesis (e.g., 6 to 8 min for the 3,290-bp product of the 604 template). It should be noted that, because displacement synthesis is on the order of 10-fold slower than nondisplacement synthesis (unpublished data), as a rough approximation we have excluded the variable contribution of single-stranded template-mediated synthesis (after opening of the circular molecules) from our calculations.

[b] Rates were calculated assuming synthesis exclusively from only one of the two nicks (unidirectional synthesis).

[c] Rates were calculated assuming simultaneous synthesis from both nicks (bidirectional synthesis)

[d] The appearance of product was judged to occur nearly coincident with one point (30 min) of the time course experiment.

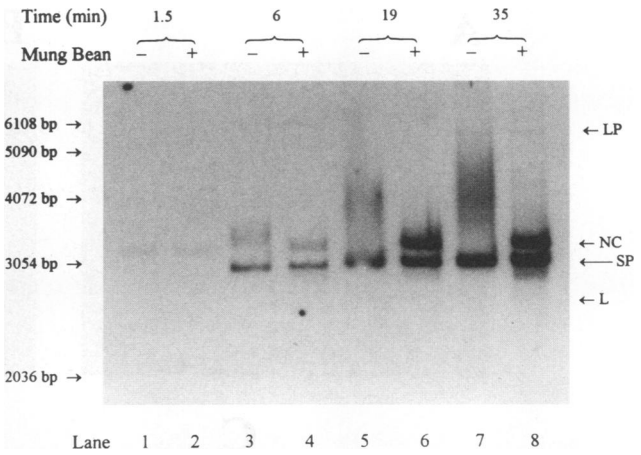

FIG. 5. Mung bean nuclease treatment of displacement synthesis intermediates. Synthesis on the 207/2479 templates was carried out in the presence of [α-^{32}P]dATP. At the indicated times, aliquots were removed and ethanol precipitated. The resulting DNA was divided into two aliquots and subjected to identical conditions plus (+) or minus (−) mung bean nuclease for 20 min at 37°C. The size markers are indicated at the left. The labels shown on the right are the same as in Fig. 4.

from the background smear of molecules with tails (see below), the linear products of successful displacement synthesis can be seen first at 8 min for the 604 template (lane 5, labeled SP for short product) and at 30 min for the 2082 template (lane 7, labeled LP for long product). Also visible in lanes 4 and 5 is a discrete product which migrated faster than the short product of displacement synthesis, yet more slowly than linear plasmid. We suspect that this band corresponds to linear intermediates which resulted from synthesis-driven opening of the circular template but which still possessed single-strand extensions. By narrowing the focus of the time course to a window centered around the earliest appearance of linear product (data not shown), we have estimated the maximum rate of displacement synthesis on four representative templates (Table 1). The calculated rate depends on whether we assume linearization occurred by synthesis from only one nick (unidirectional) or by simultaneous synthesis from both nicks (bidirectional). The maximum rates are roughly 1.5 and 0.73 nucleotides per s, respectively.

The intermediates of displacement synthesis are duplex circular molecules with either one or two growing single-stranded tails. To test the hypothesis that intermediates in the displacement reaction are nicked duplex circles containing increasingly long single-stranded tails displaced by newly synthesized DNA strands, we performed a ^{32}P-labeled time course experiment as above and treated aliquots from various time points with the single-strand-specific mung bean nuclease. Mung bean nuclease was selected because it exhibits a strong preference for single strands over nicks and thus could readily be titrated to prevent the linearization of the nicked DNAs. Figure 5 shows the results of this experiment with the 207/2479 template pair. Similar to the results shown in Fig. 4, DNA synthesis quickly converted the starting material to a heterogeneous population of molecules exhibiting decreasing mobility over time (Fig. 5, lanes 1, 3, 5, and 7). When treated with mung bean nuclease, the population was uniformly converted to a discrete ^{32}P-labeled band (Fig. 5, lanes 2, 4, 6, and 8). As predicted by the hypothesis, (i) this band comigrated with the nicked circular starting material, (ii) the amount of label incorporated into the product increased with time, and (iii) essentially none of the label incorporated into the products was lost by digestion with mung bean nuclease (compare the short product [SP] in the even and odd numbered lanes).

To directly examine the DNA intermediates and products of displacement synthesis, we have used transmission electron microscopy. Shown in Fig. 6 is the result of a representative experiment using the 207/2479 templates. Typically, a displacement synthesis reaction was stopped and spread with formamide to prevent single strand intramolecular interactions, and the DNA was stained with uranyl acetate and Pt/Pd rotary shadowed (12). In all experiments, in addition to molecules corresponding to starting material and to both types of expected linear products (data not shown), we observed a large population of circular molecules possessing either one (Fig. 6A) or two (Fig. 6B) branches or "tails." No similarly branched molecules were observed in control reaction mixtures lacking RT, indicating that we were not witnessing artifacts due to formamide-induced melting of the duplex template. It should be noted that under the conditions employed here, single-stranded DNA was extended and thickened to an extent that it was indistinguishable from duplex DNA (compare the linear double-stranded DNA with circular single-stranded DNA in Fig. 6C).

In the absence of synthesis, RT-mediated DNA unwinding is very limited. DNA helicases are characterized by their ability to promote processive, vectorial unwinding of duplex DNA in a process that is coupled to the binding and hydrolysis of nucleoside 5′-triphosphates (28). Given that RT appears to possess a helicase-like activity in addition to functioning as a DNA polymerase, we were interested in determining the extent to which the two activities are interdependent.

To address this question, we developed an assay capable of detecting RT-mediated unwinding of duplex DNA in the absence of DNA synthesis. To maximize sensitivity, we performed the assay with the 17/2669 template pair as diagrammed in Fig. 7. We specifically were interested in the 17 template, as its 3′ termini orient RT towards the small 17-bp duplex region holding together the two ends of the DNA. Thus, in addition to being susceptible to opening by a processive helicase activity, this template could also provide a means

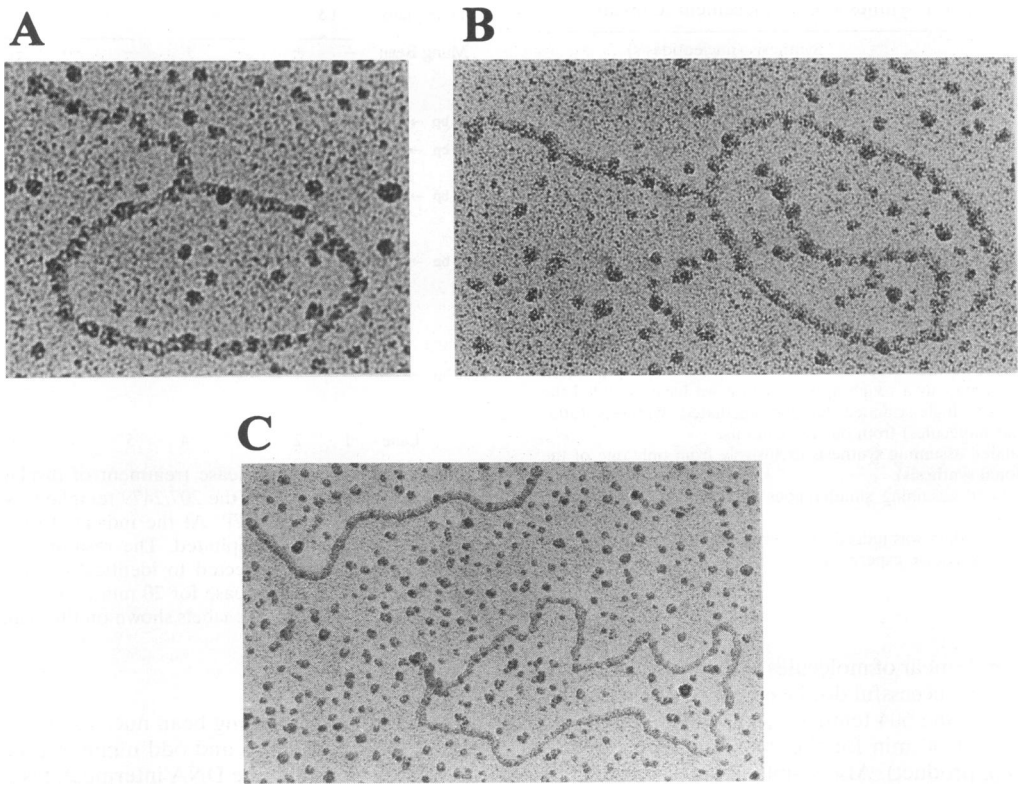

FIG. 6. Analysis of displacement synthesis intermediates by electron microscopy. Synthesis by RT on the 207/2479 templates was stopped after 30 min, and the DNA was examined by transmission electron microscopy. The spreading conditions are described in Materials and Methods. (A and B) In addition to the expected linears, a large population of circular molecules possessing either one or two branches or tails was seen. Magnification, 75,000×. (C) A mixture of linear double-stranded pUC18 and circular single-stranded M13mp9 was spread under conditions identical to those in panels A and B. Magnification, 40,000×.

for detecting a melted "footprint," or unwound region, created by a nontranslocating RT positioned at one or both 3′ termini of the DNA. It should be noted that the 17 and 2669 templates were represented equally in the mixture; we would therefore expect only one-half of the templates to be susceptible to RT-mediated melting if the orientation of the enzyme were critical (i.e., if melting occurs specifically ahead of the enzyme when positioned at a primer).

We previously had noted that under our assay conditions any melted template quickly and efficiently reannealed. Therefore, to detect what would be a transient melting event, we employed a mixture of templates linearized by two different restriction enzymes. As schematically outlined in Fig. 7, and shown in the positive controls for the experiment, melting of the 17-bp duplex at 55°C followed by quick-chilling resulted in a selective decrease in the band corresponding to the 2,686-bp linear template (Fig. 8, lane 10). As expected, the smaller fragments resulting from the unpairing of the DNA increased (these four smaller restriction fragments preexisted in the samples because linears were not separated from circles during the preparation of the DNA). Subsequent incubation under the reaction conditions resulted in the generation of unique DNA products of 3,010 and 2,362 bp due to the random sorting of the sticky-ended DNA molecules before pairing of the ends (Fig. 8, lane 11).

As shown in Fig. 8, lane 3, there was no appreciable decrease in the template band, or increase in the unique "sorted" reannealed bands, when the DNA was incubated with RT alone (compare with the RT-minus negative control in lane 2). Thus, RT, without an energy source, did not function as a helicase, nor did its binding unwind sufficient base pairs to cause melting of the remaining duplex under the conditions of the assay (see Discussion). Because the helicases characterized to date appear to couple NTP binding and hydrolysis with duplex DNA unwinding and enzyme translocation (28), we were interested in what role NTPs or dNTPs would play in the ability of RT to melt the duplex. As shown in Fig. 8, lanes 4 to 6 and 8, RT did not utilize ATP or, individually, any of the dNTPs not directly involved in synthesis as an energy source to catalyze detectable unwinding. Assuming that we could detect approximately 25 ng of product by ethidium bromide staining, we estimate that a melting event on 3% of the template molecules was the minimum level of detection in this assay.

Because synthesis on the 17 template initiates with the incorporation of five dG residues (four at the right and one at the left end [Fig. 7]), incubation of the template with RT and dGTP should allow limited synthesis, shrinking the 17-bp duplex down to 12 bp, and partially displacing the nontemplate strand. Under these conditions the template was clearly opened (the 2,686-bp band decreased by roughly one-half), as can be seen in Fig. 8, lane 7. However, no sorted, reannealed products were generated despite the opening. This result, together with the fact that the melting temperature of the 12-bp duplex is predicted to be well below 37°C, makes it likely that the product of synthesis in the presence of dGTP melted independently of any unwinding by RT. Thus, while presum-

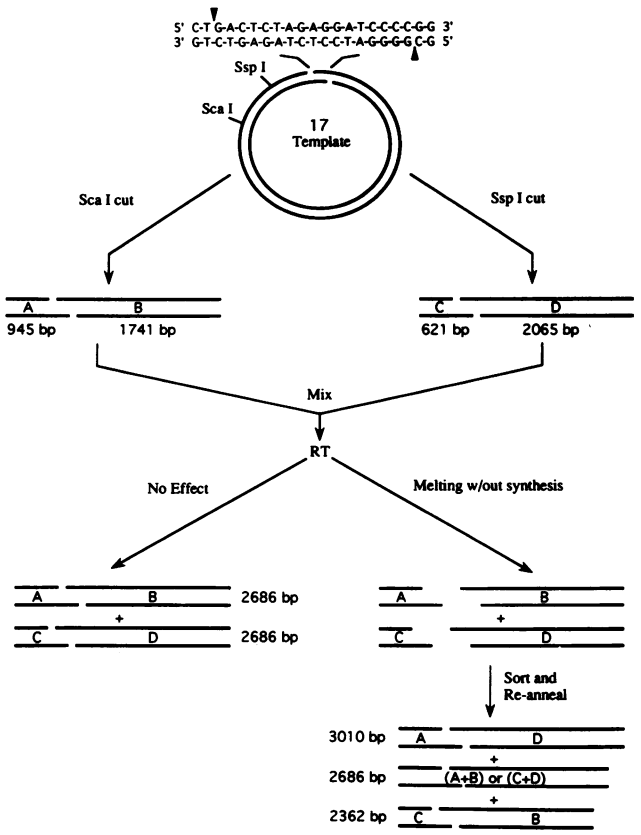

FIG. 7. Schematic representation of the assay for duplex DNA unwinding of the 17 template. The circular 17 template was cut independently with two single-site restriction enzymes (*Sca*I or *Ssp*I), and the resulting linears were mixed for the unwinding assay. Shown at the top is the sequence of the 17-bp duplex holding together the two ends of the template. Nicks are indicated by arrowheads in the sequence and by gaps in the diagram below; the 3'-hydroxyls position RT towards this 17-bp region. RT binding at the nick(s) could have no effect or could unwind the 17-bp duplex to a variable extent. In the case of DNA unwinding sufficient to cause opening of the remaining duplex (lower right), four distinct sticky-ended DNA fragments (A, B, C and D) are generated. Random sorting of these fragments before reannealing produces three linears containing 2,362, 2,686, and 3,010 bp. In contrast, if duplex unwinding is insufficient to unpair the DNA, only a 2,686-bp linear corresponding to unopened template is predicted (lower left).

ably not required in this instance, we cannot rule out the possibility that a synthesis-dependent event catalyzed a more extensive disruption of duplex template than occurred in the absence of synthesis (see Discussion).

Prompted by a previous report that AMV RT exhibits a duplex DNA unwinding-like activity independent of the presence of DNA termini to position the enzyme (11), we have examined MuLV RT for the ability to unwind duplex DNA in a primer-independent fashion. Our approach was to assay for an RT-mediated change in the superhelical nature of a covalently-closed circular duplex DNA molecule (14, 37). Since unwinding of the helix in such a molecule decreases DNA twist, the fixed relationship between DNA linking number (L), twist (T), and writhe (W), L = T + W (44), necessitates a compensatory increase in superhelicity. This effect can be detected by comparing the distribution of DNA topoisomers resulting from complete relaxation of the DNA in the presence and absence of the DNA unwinding activity. By decreasing DNA twist, a DNA unwinding protein effectively "hides" negative supercoils from relaxation by eukaryotic topoisomerase I. When the protein is removed, unwound DNA regions are allowed to reform the normal helical structure, resulting in the generation of negative supercoils (14, 37).

We examined the effects of binding to closed circular DNA by two different, displacement synthesis-competent RT preps from two different suppliers. For comparative purposes, and as a positive control, we included the unwound complex created by T7 RNA polymerase binding to its promoter in the presence of GTP. The DNA for all assays was the covalently closed plasmid, pBluescript II KS(+). Because the conditions of electrophoresis were selected to shift the distribution of relaxed topoisomers into a positively supercoiled state, the end result of any protein-mediated unwinding would be to reduce the mobility of the entire topoisomer distribution relative to that of the controls. Lanes 3 to 5 in Fig. 9 show that RT-mediated DNA unwinding, while detectable, was extremely limited (compare with negative controls [lanes 2 and 6]). Clearly, there was a gradual shift in topoisomer distribution associated with an increasing RT-to-DNA ratio. However, it was only upon reaching an enzyme-DNA molar excess of 69:1 that a shift corresponding to approximately one superhelical turn, equivalent to the unwinding of roughly 10 bp, was seen. This shift can be compared to a virtually identical change mediated by T7 RNA polymerase binding specifically to the single T7 promoter region on the plasmid (lane 8 versus T7-minus negative controls, lanes 7 and 9). We have not independently determined the fraction of active RT molecules in our commercially supplied RT preparations; this precludes a quantitative determination of the unwound region per enzyme. However, by assuming that binding sites were not limiting, we estimate that RT-mediated unwinding must have been very low. If greater than 10 of the possible 69 enzyme molecules (an active proportion of roughly 14%) were capable of binding the template in this assay, unwinding would necessarily have been less than 1 bp per molecule. It seems most likely, therefore, that RT binding, rather than dissociating base pairs, had a more subtle effect on DNA twist. At high RT/DNA ratios this effect, cumulatively, was detectable as a slight amount of unwinding by this assay. While subtle, the effect was associated specifically with RT because BSA at a 90:1 molar excess did not demonstrate a similar effect on DNA twist (lanes 2 and 6), and controls ruled out any effect ascribable to the RT storage buffer (data not shown). An identical pattern was seen whether RT interacted with negatively supercoiled DNA or with DNA which had been relaxed by topoisomerase I before binding (data not shown). Thus, it appears that the binding effect seen was not the result of RT binding specifically to single-stranded regions created on the underwound form I DNA.

A 181-amino-acid C-terminal truncation of RT displays dramatically reduced strand displacement activity. While the DNA polymerase and RNase H activities of M-MuLV RT are contained within a single polypeptide chain, their respective catalytic sites reside in physically and functionally separable domains of the protein: DNA polymerase activity is found in the N terminus, while RNase H activity lies in the C terminus (39). As a first approach to address whether the structural determinants of displacement synthesis reside along with the polymerase domain in the N-terminal portion of RT, we examined the displacement synthesis activity of BRL Superscript I. This enzyme possesses a functional DNA polymerase domain but lacks detectable RNase H activity because of a

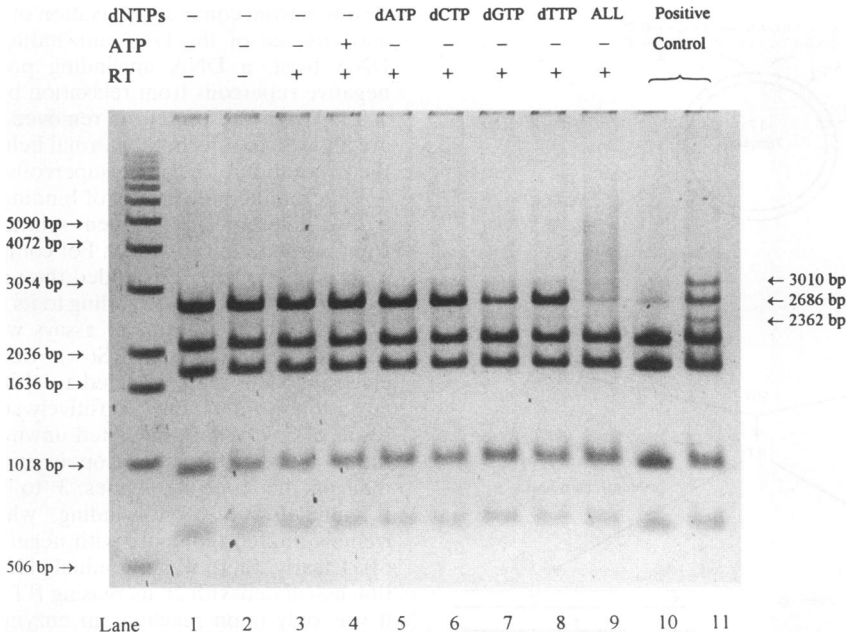

FIG. 8. Duplex DNA unwinding assay on the 17 template. RT was assayed for a duplex DNA unwinding activity as outlined schematically in Fig. 7. The 17/2669 template pair was incubated without RT (lane 2) or with RT (lanes 3 to 9) under the conditions indicated at the top for 30 min at 37°C. Lane 1 was loaded without incubation. The positive control in lane 10 was subjected to heat denaturation at 55°C in TE and quick-chilled before loading. The positive control in lane 11 was similarly denatured and then incubated with RT and RT buffer in conjunction with the samples from lanes 2 to 9 (lane 11). The three bands of interest in this assay are indicated by arrows at the right. The 2,686-bp band corresponds to the linearized 17/2669 templates; the 2,362- and 3,010-bp bands are generated specifically by a melting-reannealing event. Size markers are indicated at the left. The four smaller bands correspond to DNA fragments preexisting in the samples (see text).

C-terminal truncation of 181 amino acids (26). As shown in Fig. 10, the carboxy-terminal 181 amino acids were clearly not required for at least limited strand displacement synthesis. However, relative to the wild-type enzyme, the truncated protein demonstrated a dramatically reduced displacement synthesis capability. On the 117/2569 template pair, the truncated protein synthesized approximately fourfold-less short product than the wild type and produced no long product during the 1.5-h incubation (Fig. 10A, lane 3 versus lane 2). When analyzed by a ^{32}P-labeled time course experiment using the 207/2479 template pair, the truncated protein again demonstrated only limited displacement synthesis ability, failing to complete 207 bp of synthesis during the 60-min incubation (Fig. 10B). These data indicate a maximum rate of displacement synthesis by the mutant enzyme of less than 0.06 nucleotides per s, which is at least an order of magnitude slower than the wild-type enzyme (see above) (Table 1). We have compared synthesis on single- and double-stranded templates by the truncated enzyme and find the defect to be specific for strand displacement synthesis (data to be published elsewhere). The absence of a functional RNase H activity in Superscript I (26) appears to be unrelated to its strand displacement synthesis characteristics, as subsequent experiments utilizing BRL Superscript II, a multiple point mutant RNase H$^-$ enzyme, demonstrated a displacement synthesis activity identical to that of the wild-type enzyme (data not shown).

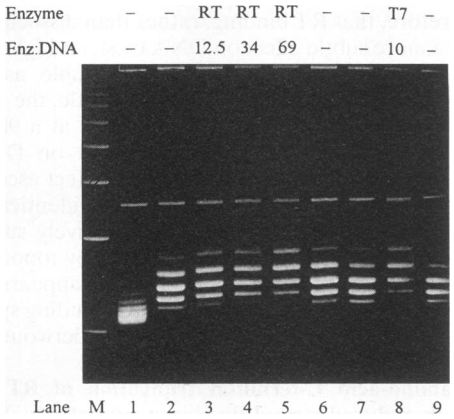

FIG. 9. Assay for RT-induced unwinding of duplex DNA in the absence of a primer terminus. Agarose gel analysis of pBluescript II KS(+) DNAs followed relaxation by eukaryotic topoisomerase I (lanes 2 to 9). The DNA was incubated under RT conditions (see Materials and Methods) with a 90:1 molar excess of BSA (lanes 2 and 6) or the indicated molar excess of RT (lanes 3 to 5) before relaxation with topoisomerase I. The enzyme (Enz) was M-MuLV RT (lanes 3 and 4) or Superscript II (lane 5). The DNA was incubated under T7 RNA polymerase conditions (see Materials and Methods) without (lanes 7 and 9) or with (lane 8) the indicated molar excess of T7 RNA polymerase before relaxation with topoisomerase I. Lane 1 shows untreated superhelical plasmid DNA.

DISCUSSION

The precise mechanism by which strand displacement synthesis is achieved during reverse transcription has been unclear. While the viral RT has remained an attractive candidate because of its integral role in reverse transcription, evidence to date has failed to demonstrate sufficient RT-associated displacement synthesis to meet the in vivo requirement. To readdress this issue, we constructed 10 nicked circular duplex

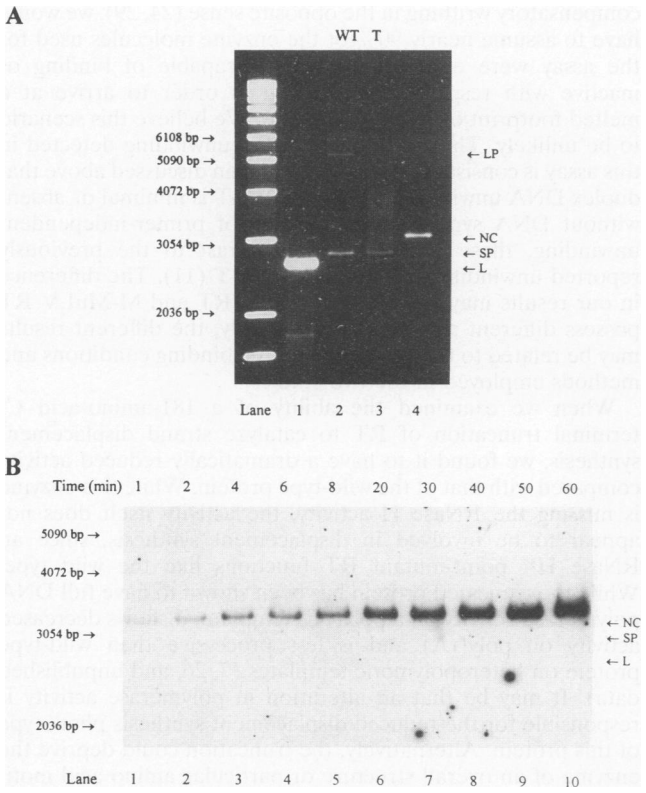

FIG. 10. Displacement synthesis by a 181-amino-acid C-terminal truncation of RT. (A) Synthesis on the 117/2569 template pair was essentially as described in Materials and Methods for RT-mediated displacement synthesis, except the DNA amount was approximately 100 ng and the incubation time was 1.5 h. Synthesis was carried out by either wild-type (WT) enzyme (lane 2) or the truncated (T) enzyme (lane 3). Lane 1 shows linearized template; lane 4 shows template incubated without RT. The labels at the right are the same as for Fig. 4. The sizes of the DNA markers are indicated at the left. (B) A time course of synthesis by the truncated enzyme on the 207/2479 template pair in the presence of [α-^{32}P]dATP was carried out as described in Materials and Methods. The labels at the right are the same as for Fig. 4. The positions of size markers are indicated at the left.

DNA templates to serve as substrates for displacement synthesis by purified M-MuLV RT. On all 10 templates, ranging from 17 through 2,669 bp, RT was capable of completing synthesis as indicated by the generation of linear products of the predicted structure and size. The intermediates of synthesis, as examined by [α-^{32}P]dATP incorporation, mung bean nuclease sensitivity, and direct visualization by electron microscopy, were nicked duplex circles with single-stranded tails. The experiments described here indicate that purified M-MuLV RT is capable of displacing the nontemplate strand during synthesis in vitro to an extent much greater than would be required for the completion of the LTRs following the second strand transfer reaction of reverse transcription. Because additional strand displacement of DNA is probably not required (see below) (4) and because strand displacement of RNA would be greatly facilitated by the RNase H activity of RT (21), the displacement synthesis capability demonstrated here for M-MuLV RT may be sufficient to meet all of the in vivo requirements. To our knowledge, this is the first demonstration of such a striking displacement synthesis activity in a retroviral RT. While we have not excluded the possibility that accessory factors of viral or cellular origin facilitate strand displacement synthesis during reverse transcription in vivo, for M-MuLV at least, it appears such aid is not required.

The maximum rate of displacement synthesis on four representative templates was estimated by performing a time course experiment in the presence of [α-^{32}P]dATP. Depending upon whether one assumes unidirectional or bidirectional synthesis on the templates, the estimated maximum rate falls between 0.73 and 1.5 nucleotides per s. This rate is roughly 10-fold slower than nondisplacement synthesis by M-MuLV RT on a heteropolymeric DNA template in vitro (our unpublished data), and 10- to 20-fold slower than the published incorporation rate of HIV-1 RT on homopolymeric and heteropolymeric RNA templates in vitro (21, 34). As noted above, it is clear that displacement synthesis through the ~600-bp LTR region is required for completion of reverse transcription following the second jump; in principle, this synthesis could be performed by one RT extending the minus DNA strand or by two RTs simultaneously extending both the minus and plus strands. Plus-strand synthesis from multiple start sites would be expected to lead to downstream displacement, as has been documented in the ASLV system; however, completion of this displacement, in principle, should not be obligatory for viral replication, since a mature plus strand could be generated by nuclease digestion of any displaced single-stranded tails followed by ligation of the resulting discontinuous plus strand (4). It is uncertain whether strand displacement synthesis would be rate limiting for completion of the last step of reverse transcription. If the entire plus strand is synthesized from one initiation event, as is generally depicted, our calculated rates suggest that displacement synthesis by the minus strand through the LTR region need not be rate limiting (594 bp of displacement synthesis versus 8,246 nucleotides of single strand template directed synthesis to complete the 8,858-bp linear duplex) (38). However, if plus strands are synthesized from two or more start sites (2, 3, 10, 13, 17, 19, 23, 27, 33) and a continuous plus strand is generated by ligation, it may be that displacement synthesis through the LTR is the rate limiting event once the second jump has occurred.

It appears that the DNA unwinding activity of RT cannot be functionally uncoupled from DNA synthesis and thus that RT does not function as a classical helicase. We investigated synthesis-independent DNA unwinding by RT in two distinct settings: on a nicked template, we looked for melting downstream of a primer-positioned RT, and on a closed circular duplex molecule we examined the ability of RT to unwind duplex DNA independently of the presence of termini. Our assay in the former case took advantage of the fact that the two ends of the 17 template are held together by only 17 bp of duplex DNA. RT is oriented by the 3′-hydroxyls of this DNA towards the 17-bp region; therefore, a detectable melted footprint would arise if a primer-positioned RT unwound sufficient downstream DNA to cause unpairing of the remaining duplex. To define what would be a detectable footprint in our assay, we used an experimentally determined melting temperature for the starting template (56°C), the nearest-neighbor model of Borer et al. (5, 35), and the thermodynamic values of Breslauer et al. (6) to calculate the predicted unpairing temperature of the 17 template after an unwinding event initiated from either one or both nicks in the DNA. Our analysis predicts that an unwinding event of greater than 2 bp would be detectable at the 37°C assay temperature if RT were positioned at both termini or solely at the right one, while unwinding specifically at the left nick would be detectable if the extent were greater than 6 bp. Under no conditions did we detect a melting event without concomitant DNA synthesis,

and we noted no difference between the presence and the absence of a hydrolyzable NTP or dNTP source unless it was the particular dNTP encoded by the template strand. As there is no a priori reason to assume that RT would be preferentially directed to the left terminus over the right, or that simultaneous binding of RT to both termini would be sterically precluded (22, 31), we conclude that independent of DNA synthesis, RT-mediated unwinding is minimal or absent.

Lohman has described a potential mechanism of helicase-catalyzed DNA unwinding, classified as passive, in which the enzyme stabilizes transiently generated single-stranded DNA rather than actively participating in the unwinding event (28). While he noted that no direct evidence exists to support such a mechanism, it is possible that RT functions in this manner. Thus, one model for RT-mediated unwinding would have RT functioning to bind single strands generated by breathing or fraying of the duplex at the transition from single- to double-stranded DNA. This destabilization of the duplex would in turn facilitate synthesis-driven translocation of the enzyme through regions of double-stranded DNA. Alternatively, RT may employ an active mechanism for DNA unwinding (28). It is proposed that helicases actively destabilize duplex DNA by coupling conformational changes in the protein to NTP binding or hydrolysis (28). In an analogous manner, RT could utilize a conformational change linked to binding of the template-encoded dNTP or to the formation of the phosphodiester bond during chain elongation, to actively destabilize duplex DNA in front of the enzyme. Because the 17 template encodes five dG residues upon the initiation of synthesis, we predict that the product resulting from incubation of the template with RT and dGTP should melt independently of any DNA unwinding activity. Thus, our data neither favor nor exclude the possibility that an event exclusive to DNA synthesis catalyzes an active disruption of duplex template by RT or that this disruption could be greater than the maximum of 2 bp seen in the absence of synthesis. We are currently examining this possibility. It should be noted, however, that the discrepancy we observe between the rate of displacement and nondisplacement synthesis on an otherwise identical DNA template (see above) favors a model of displacement synthesis in which the act of strand separation is rate limiting. These data would appear to be more consistent with a passive or limited active unwinding mechanism by RT than with a robust active mechanism such as is observed for true DNA helicases. Additionally, because RT is constrained by synthesis to translocate in steps of one nucleotide, simple economy might dictate that unwinding be on a similar scale.

Because AMV RT has previously been reported to possess a duplex DNA unwinding activity which functions independently of synthesis and of the presence of a DNA terminus to position the enzyme (11), we examined M-MuLV RT for a similar capability. To address primer-independent DNA unwinding, we assayed for an RT-mediated change in the superhelical nature of a covalently closed circular duplex molecule. This method has previously been used to determine the size of the unwound region created by *E. coli* RNA polymerase and calf thymus RNA polymerase II at their respective promoters (14, 37), as well as by *Xenopus* transcription factor A (16). While we detected a reproducible effect on DNA twist, it appears unlikely that RT is capable of unwinding even 1 bp by binding to strictly duplex DNA: it was only at an enzyme-DNA molar excess of 69:1 that we detected a shift corresponding to the unwinding of 10 bp. At a minimum, then, RT binding could effect a net unwinding of the duplex of only 5°. Since it is unlikely that RT binding to the DNA was limited by the availability of sites or that RT balances duplex unwinding with compensatory writhing in the opposite sense (24, 29), we would have to assume nearly 90% of the enzyme molecules used for the assay were either functionally incapable of binding or inactive with respect to unwinding in order to arrive at a melted footprint of 1 bp per enzyme. We believe this scenario to be unlikely. Thus, the extent of the unwinding detected in this assay is consistent with the conclusion discussed above that duplex DNA unwinding by M-MuLV RT is minimal or absent without DNA synthesis. In the case of primer-independent unwinding, these data stand in contrast to the previously reported unwinding activity of AMV RT (11). The difference in our results may indicate that AMV RT and M-MuLV RT possess different activities. Alternatively, the different results may be related to the differences in the binding conditions and methods employed in the two studies.

When we examined the ability of a 181-amino-acid C-terminal truncation of RT to catalyze strand displacement synthesis, we found it to have a dramatically reduced activity compared with that of the wild-type protein. While this enzyme is missing the RNase H activity, the activity itself does not appear to be involved in displacement synthesis, since an RNase H^- point-mutant RT functions like the wild type. While the truncated protein has been shown to have full DNA polymerase activity on a poly(rC) template, it shows decreased activity on poly(rA) and is less processive than wild-type protein on heteropolymeric templates (7, 26, and unpublished data). It may be that an alteration in polymerase activity is responsible for the reduced displacement synthesis phenotype of this protein. Alternatively, the truncation could deprive the enzyme of an overall structure or particular amino acid motif required for efficient displacement synthesis. On this note, it is interesting that while native M-MuLV RT has been reported to dimerize upon binding to primer template, mutant RTs missing the RNase H domain C helix or truncated from the RNase H domain through the C terminus failed to dimerize (41). All DNA helicases characterized to date appear to function in oligomeric form, and the presence of at least two DNA-binding sites is thought to be required for an active DNA unwinding mechanism (28).

How closely do our templates approximate an in vivo intermediate of reverse transcription? The exact nature of the DNA intermediate produced by the second strand transfer reaction of reverse transcription is not known. While the molecule is commonly depicted with a nearly complete minus strand and a much shorter strong-stop plus strand (as shown in Fig. 1D), the in vivo intermediate may be more complex (4). While analogous to the structure in Fig. 1D, our templates more closely model the intermediate which would precede the complete linear DNA product of reverse transcription if plus-strand and minus-strand DNA synthesis into the LTR region occurred coincidentally. In principle, such an intermediate could arise by two distinct mechanisms. Subsequent to the second jump, if plus-strand extension were to proceed much more rapidly than minus-strand extension, the "correct" PPT-primed plus strand could reach the LTR before the minus strand was complete. Our estimates of the relative rates of displacement and nondisplacement synthesis (see above) suggest that this event is possible. More likely is the possibility that a secondary plus strand initiated upstream of the PPT could reach the U3 region and commence displacement synthesis concurrent with minus-strand extension into the U5 region. Consistent with this possibility, evidence suggests that viruses such as ASLV (3, 19, 23, 40), HIV-1 (9, 10), visna virus (2, 17), spumavirus (27, 42), and M-MuLV (13, 33) utilize upstream, secondary sites to prime plus-strand synthesis.

Interestingly, this convergent displacement synthesis could,

in principle, be problematic for RT. Depending on how RT translocates along the template, the potential exists for the development of topological problems between the approaching synthesis forks. If RT tracks along the helix, rotating once per helical turn, one would expect the displaced single strands to remain helically wound around the duplex behind the enzyme. Under these conditions, there should be no topological problem associated with elongation (25). However, if RT were constrained to prevent free rotation and the displaced strands pushed away from the template as the enzyme advanced, one would expect the generation of positive supercoils ahead of the synthesis fork (25). This overwinding should be inhibitory to synthesis unless alleviated by some mechanism; in vitro this would most likely be achieved by passage (unwinding) of the displaced single strands around the template. The preferential stalling of RT on the longer displacement templates could be accounted for by the generation of torsional strain or by an inability of the longer displaced strands to unwind around the template. However, this stalling could also be accounted for by an increased likelihood of the enzyme encountering a sequence inhibitory to polymerization or strand displacement on the longer templates (36). The free single strands seen in our electron micrographs do not necessarily favor one mechanism over the other, as thermal motion and entropy would drive the gradual unwinding of displaced strands left helically wound around the duplex during synthesis. Therefore, at least in the in vitro reaction on these templates, we favor the simpler model whereby a freely rotating RT prevents the generation of topological problems during convergent displacement synthesis. The observed constant maximum rate of displacement synthesis over the range from 604 to 2,669 bp is consistent with this mechanism functioning on at least a subset of the templates.

ACKNOWLEDGMENTS

This work was supported by a grant from the National Institutes of Health (CA51605). S.H.W. is supported by the Medical Scientist Training Program (5T32GM07266) of the National Institutes of Health and a fellowship from the Poncin Scholarship Fund.

We thank Stephanie Lara and Jimmie Lara for assistance with the electron microscopy; Lance Stewart for kindly providing purified recombinant human topoisomerase I; and Caterina Randolph, Lance Stewart, and Sharon Schultz for helpful discussions and review of the manuscript. S.H.W. thanks Eric "SB" Barklis for the Pigmania lessons.

REFERENCES

1. **Ausubel, F. M., R. Brent, R. E. Kingston, D. D. Moore, J. G. Seidman, J. A. Smith, and K. Struhl (ed.).** 1987. Current protocols in molecular biology. John Wiley & Sons, Inc., New York.
2. **Blum, H. E., J. D. Harris, P. Ventura, D. Walker, K. Staskus, E. Retzel, and A. Haase.** 1985. Synthesis in cell culture of the gapped linear duplex DNA of the slow virus visna. Virology **142:**270–277.
3. **Boone, L. R., and A. M. Skalka.** 1981. Viral DNA synthesized in vitro by avian retrovirus particles permeabilized with mellitin: evidence for a strand displacement mechanism in plus-strand synthesis. J. Virol. **37:**117–126.
4. **Boone, L. R., and A. M. Skalka.** 1993. Strand displacement synthesis by reverse transcriptase, p. 119–134. *In* A. M. Skalka and S. P. Goff (ed.), Reverse transcriptase. Cold Spring Harbor Laboratory Press, Cold Spring Harbor, N.Y.
5. **Borer, P. N., B. Dengler, I. Tinoco, Jr., and O. Uhlenbeck.** 1974. Stability of ribonucleic acid double-stranded helices. J. Mol. Biol. **86:**843–853.
6. **Breslauer, K. J., R. Frank, H. Blocker, and L. A. Marky.** 1986. Predicting DNA duplex stability from the base sequence. Proc. Natl. Acad. Sci. USA **83:**3746–3750.
7. **Buiser, R. G., J. J. DeStefano, L. M. Mallaber, F. J. Fay, and R. A. Bambara.** 1991. Requirements for the catalysis of strand transfer synthesis by retroviral DNA polymerases. J. Biol. Chem. **266:** 13103–13109.
8. **Champoux, J. J.** 1993. Roles of ribonuclease H in reverse transcription, p. 103–118. *In* A. M. Skalka and S. P. Goff (ed.), Reverse transcriptase. Cold Spring Harbor Laboratory Press, Cold Spring Harbor, N.Y.
9. **Charneau, P., M. Alizon, and F. Clavel.** 1992. A second origin of DNA plus-strand synthesis is required for optimal human immunodeficiency virus replication. J. Virol. **66:**2814–2820.
10. **Charneau, P., and F. Clavel.** 1991. A single-stranded gap in human immunodeficiency virus unintegrated linear DNA defined by a central copy of the polypurine tract. J. Virol. **65:**2415–2421.
11. **Collett, M. S., J. P. Leis, M. S. Smith, and A. J. Faras.** 1978. Unwinding-like activity associated with avian retrovirus RNA-directed DNA polymerase. J. Virol. **26:**498–509.
12. **Davis, R. W., M. Simon, and N. Davidson.** 1971. Electron microscope heteroduplex methods for mapping regions of base sequence homology in nucleic acids. Methods Enzymol. **21:**413–428.
13. **DesGroseillers, L., E. Rassart, M. Zollinger, and P. Jolicoeur.** 1982. Synthesis of murine leukemia viral DNA in vitro: evidence for plus-strand DNA synthesis at both ends of the genome. J. Virol. **42:**326–330.
14. **Gamper, H. B., and J. E. Hearst.** 1983. Size of the unwound region of DNA in Escherichia coli RNA polymerase and calf thymus RNA polymerase II ternary complexes. Cold Spring Harbor Symp. Quant. Biol. **47:**455–461.
15. **Gilboa, E., S. W. Mitra, S. Goff, and D. Baltimore.** 1979. A detailed model of reverse transcription and tests of crucial aspects. Cell **18:**93–100.
16. **Hanas, J. S., D. F. Bogenhagen, and C.-W. Wu.** 1984. DNA unwinding ability of Xenopus transcription factor A. Nucleic Acids Res. **12:**1265–1277.
17. **Harris, J. D., J. V. Scott, B. Traynor, M. Brahic, L. Stowring, P. Ventura, A. T. Hasse, and R. Peluso.** 1981. Visna virus DNA: discovery of a novel gapped structure. Virology **113:**573–583.
18. **Hottiger, M., V. N. Podust, R. L. Thimmig, C. McHenry, and U. Hubscher.** 1994. Strand-displacement activity of the human immunodeficiency virus type 1 reverse transcriptase heterodimer and its individual subunits. J. Biol. Chem. **269:**986–991.
19. **Hsu, T. W., and J. M. Taylor.** 1982. Single-stranded regions on unintegrated avian retrovirus DNA. J. Virol. **44:**47–53.
20. **Hu, W.-S., and H. M. Temin.** 1990. Retroviral recombination and reverse transcription. Science **250:**1227–1233.
21. **Huber, H. E., J. M. McCoy, J. S. Seehra, and C. C. Richardson.** 1989. Human immunodeficiency virus 1 reverse transcriptase: template binding, processivity, strand displacement synthesis, and template switching. J. Biol. Chem. **264:**4669–4678.
22. **Jacobo-Molina, A., J. Ding, R. G. Nanni, A. D. Clark, Jr., X. Lu, C. Tantillo, R. Williams, G. Kamer, A. Ferris, P. Clark, A. Hizi, S. Hughes, and E. Arnold.** 1993. Crystal structure of human immunodeficiency virus type 1 reverse transcriptase complexed with double-stranded DNA at 3.0 A resolution shows bent DNA. Proc. Natl. Acad. Sci. USA **90:**6320–6324.
23. **Junghans, R. P., L. R. Boone, and A. M. Skalka.** 1982. Products of reverse transcription in avian retrovirus analyzed by electron microscopy. J. Virol. **43:**544–554.
24. **Kim, Y., J. H. Geiger, S. Hahn, and P. B. Sigler.** 1993. Crystal structure of yeast TBP/TATA-box complex. Nature (London) **365:**512–520.
25. **Kornberg, A., and T. A. Baker.** 1992. DNA replication. W. H. Freeman and Co., New York.
26. **Kotewicz, M. L., C. M. Sampson, J. M. D'Alessio, and G. F. Gerard.** 1988. Isolation of cloned moloney murine leukemia virus reverse transcriptase lacking ribonuclease H activity. Nucleic Acids Res. **16:**265–277.
27. **Kupiec, J. J., J. Tobaly-Tapiero, M. Canivet, M. Santilla-Hayat, R. M. Flugel, J. Peries, and R. Emanoil-Ravier.** 1988. Evidence for a gapped linear duplex DNA intermediate in the replicative cycle of human and simian spumaviruses. Nucleic Acids Res. **16:**9557–9565.
28. **Lohman, T. M.** 1993. Helicase-catalyzed DNA unwinding. J. Biol. Chem. **268:**2269–2272.
29. **Lorch, Y., and R. D. Kornberg.** 1993. Near-zero linking difference

upon transcription factor IID binding to promoter DNA. Mol. Cell. Biol. **13:**1872–1875.
30. **Matson, S., P. Fay, and R. Bambara.** 1980. Mechanism of inhibition of the avian myeloblastosis virus deoxyribonucleic acid polymerase by adriamycin. Biochemistry **19:**2089–2096.
31. **Metzger, W., T. Hermann, O. Schatz, S. F. J. Le Grice, and H. Heumann.** 1993. Hydroxyl radical footprint analysis of human immunodeficiency virus reverse transcriptase-template primer complexes. Proc. Natl. Acad. Sci. USA **90:**5909–5913.
32. **Ratner, L., W. Haseltine, R. Patarca, K. J. Livak, B. Starcich, S. F. Josephs, E. R. Doran, J. A. Rafalski, E. A. Whitehorn, K. Baumeister, L. Ivanoff, S. R. Petteway, Jr., M. L. Pearson, J. A. Lautenberger, T. S. Papas, J. Ghrayeb, N. T. Chang, R. C. Gallo, and F. Wong-Staal.** 1985. Complete nucleotide sequence of the AIDS virus, HTLV-III. Nature (London) **313:**277–284.
33. **Rattray, A. J., and J. J. Champoux.** 1987. The role of Moloney murine leukemia virus RNase H activity in the formation of plus-strand primers. J. Virol. **61:**2843–2851.
34. **Reardon, J. E.** 1992. Human immunodeficiency virus reverse transcriptase: steady state and pre-steady-state kinetics of nucleotide incorporation. Biochemistry **31:**4473–4479.
35. **Rychlik, W., W. J. Spencer, and R. E. Rhoads.** 1990. Optimization of the annealing temperature for DNA amplification in vitro. Nucleic Acids Res. **18:**6409–6412.
36. **Samadashwily, G. M., A. Dayn, and S. M. Mirkin.** 1993. Suicidal nucleotide sequences for DNA polymerization. EMBO J. **12:** 4975–4983.
37. **Saucier, J.-M., and J. C. Wang.** 1972. Angular alteration of the DNA helix by E. coli RNA polymerase. Nature (London) New Biol. **239:**167–170.
38. **Shinnick, T. M., R. A. Lerner, and J. G. Sutcliffe.** 1981. Nucleotide sequence of Moloney murine leukemia virus. Nature (London) **293:**543–548.
39. **Tanese, N., and S. P. Goff.** 1988. Domain structure of the Moloney murine leukemia virus reverse transcriptase: mutational analysis and separate expression of the DNA polymerase and RNase H activities. Proc. Natl. Acad. Sci. USA **85:**1777–1781.
40. **Taylor, J. M., A. Cywinski, and J. K. Smith.** 1983. Discontinuities in DNA synthesized by an avian retrovirus. J. Virol. **48:**654–659.
41. **Telesnitsky, A., and S. P. Goff.** 1993. RNase H domain mutations affect the interaction between moloney murine leukemia virus reverse transcriptase and its primer template. Proc. Natl. Acad. Sci. USA **90:**1276–1280.
42. **Tobaly-Tapiero, J., J. J. Kupiec, M. Santillana-Hayat, M. Canivet, J. Peries, and R. Emanoil-Raiver.** 1991. Further characterization of the gapped DNA intermediates of human spumavirus: evidence for a dual initiation of plus-strand DNA synthesis. J. Gen. Virol. **72:**605–608.
43. **Varmus, H., and P. Brown.** 1989. Retroviruses, p. 53–108. *In* D. E. Berg and M. M. Howe (ed.), Mobile DNA. American Society for Microbiology, Washington, D.C.
44. **Vinograd, J., J. Lebowitz, and R. Watson.** 1968. Early and late helix-coil transitions in closed circular DNA. The number of superhelical turns in polyoma DNA. J. Mol. Biol. **33:**173–197.